

Enhanced Cooper pairing versus suppressed phase coherence shaping the superconducting dome in coupled aluminum nanograins

Uwe S. Pracht,¹ Nimrod Bachar,^{2,3,4} Lara Benfatto,⁵ Guy Deutscher,³ Eli Farber,² Martin Dressel,¹ and Marc Scheffler^{1,*}

¹*Physikalisches Institut, Universität Stuttgart, Germany*

²*Laboratory for Superconductivity and Optical Spectroscopy, Ariel University, Israel*

³*Raymond and Beverly Sackler School of Physics and Astronomy, Tel Aviv University, Israel*

⁴*Department of Quantum Matter Physics, University of Geneva, Switzerland*

⁵*ISC-CNR and Department of Physics, Sapienza University of Rome, Italy*

(Received 30 October 2015; published 21 March 2016)

The development of the fundamental superconducting (SC) energy scales—the SC energy gap Δ and the superfluid stiffness J —of granular aluminum, i.e., thin films composed of coupled nanograins, is studied by means of optical THz spectroscopy. Starting from well-coupled grains, Δ grows as the grains are progressively decoupled, causing the unconventional increase of T_c with sample resistivity. When the grain coupling is suppressed further, Δ saturates while the critical temperature T_c decreases, concomitantly with a sharp decline of J , delimiting a SC dome in the phase diagram. This crossover to a phase-driven SC transition is accompanied by an optical gap surviving into the normal state above T_c . We demonstrate that granular aluminum is an ideal testbed to understand the interplay between quantum confinement and global SC phase coherence due to nanoinhomogeneity.

DOI: [10.1103/PhysRevB.93.100503](https://doi.org/10.1103/PhysRevB.93.100503)

Deterministic enhancement of the superconducting (SC) critical temperature T_c is a long-standing goal in solid-state physics. In a large variety of SC systems [1–5], the initial enhancement via tuning of a control parameter is followed by a suppression of T_c , shaping a superconducting dome in the phase diagram. Although popular for high- T_c cuprate SC, the first appearance of a SC dome dates back to the late 1960s [6–8] in granular Al, i.e., thin films composed of grains, in our case with 2 nm diameter, separated by thin insulating barriers. The coupling between the grains can be controlled during film growth, leading to samples with strong coupling and low resistivity (LR) in electrical transport, compared to high resistivity (HR) samples with weak intergrain coupling. In LR samples T_c can be *enhanced* up to several times the bulk-value T_{c0} , whereas it is suppressed to zero in HR samples, see Fig. 1(a).

Though being known for half a century, and despite several theoretical proposals [9–14], the underlying mechanism enhancing T_c in granular Al has not been identified yet. On general grounds, T_c is controlled by the energy scales associated with the amplitude and phase of the complex SC order parameter $\psi = \Delta e^{i\phi}$. While the SC energy gap Δ measures the pairing strength between the electrons, the rigidity of the collective phase-coherent state, responsible for the superfluid behavior, is measured by the superfluid stiffness J . In ordinary BCS superconductors, e.g., bulk Al, J exceeds Δ by orders of magnitudes, and the SC transition at T_c is amplitude driven. On the other hand, if one can suppress J below Δ , the transition is expected to be phase driven, due to the loss of phase coherence at a temperature scale of order of J [15]. In isolated tin nanoparticles [16] the enhanced Δ can be understood as a consequence of finite-size effects [9–14]. In practice for sufficiently small isolated grains the continuous bulk DOS becomes discrete and one can observe

the electronic shell effect, resulting in a density-of-states (DOS) enhancement at E_F [11–14]. However, it has not been experimentally established whether such a mechanism can explain also the increase of the global T_c in dense grain arrays, since here the grain coupling affects Δ and J in a competing fashion. Indeed, in the LR regime the coupling between grains smears out the local DOS [17], smoothing the quantum confinement in each grain and its effect of the T_c enhancement. In addition, in the HR regime where the grains are progressively decoupled charging effects can ultimately overcome the Josephson coupling between grains and suppress the SC state via the reduction of J , in full analogy with what observed, e.g., in granular lead [18–20], or artificial arrays of widely spaced SC nanodots [21–23], where the global T_c never exceeds the one of the bulk constituent.

The above scenario implies that HR granular Al should undergo a direct superconductor-insulator transition (SIT), analogous to homogeneously disordered films of conventional superconductors, like, e.g., NbN, TiN, and InO_x [18,19], or artificial LAO/STO heterostructures [24]. This analogy is made more interesting by the recent observation that in homogeneously disordered films [25–30] and LAO/STO interfaces [24] the SC properties become spatially inhomogeneous near the SIT. In this respect, the emergent granularity, either intrinsic or extrinsic, would constitute a general mechanism for the formation of superconductivity from an almost insulating normal state. In order to outline these potential analogies, and to understand the origin of the SC dome in granular Al, we use optical spectroscopy to assess the evolution of the characteristic SC energy scales as a function of grain coupling, which so far has been only partly explored [7,31–37]. We show that, starting from well-coupled grains, Δ grows with progressive grain decoupling, causing the increasing of T_c . As the grain coupling is suppressed further, Δ saturates while T_c decreases, concomitantly with a sharp decline of J . This crossover to a phase-driven SC transition is accompanied by an optical gap persisting above T_c . Our findings identify granular

*marc.scheffler@pi1.physik.uni-stuttgart.de

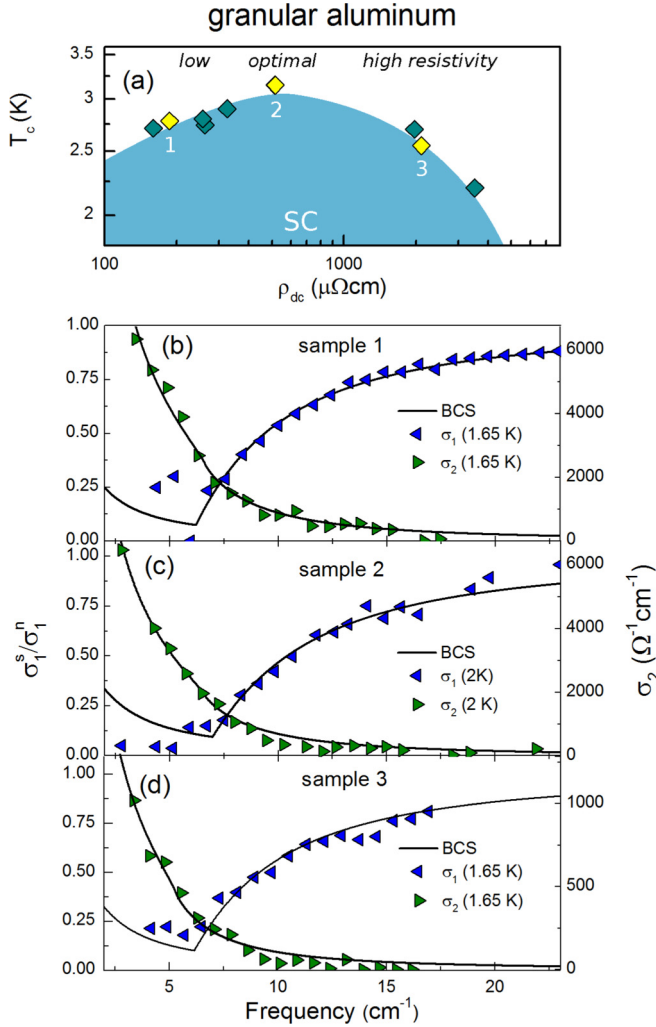


FIG. 1. Superconducting dome and dynamical conductivity. (a) Critical temperature T_c as a function of the normal-state resistivity (measured at 5 K) of granular Al films studied in this work. Yellow symbols refer to the samples displayed in panels below. T_c encloses a dome-like superconducting phase with low-, optimal- and high-resistivity regimes. (b)–(d) (Normalized) spectra of $\sigma_1(\nu)$ and $\sigma_2(\nu)$ of samples located on the left (sample 1), the right (sample 3), and at the maximum (sample 2) of the SC dome. The solid lines are fits to the Mattis-Bardeen theory. Note that the fit on σ_1 disregards the low-frequency range due to excessive conductivity beyond Mattis-Bardeen theory.

Al as an ideal testbed to understand the basic mechanisms for enhancement and suppression of superconductivity due to nanoinhomogeneity.

Thin films of 40 nm thickness were thermally evaporated on $10 \times 10 \times 2 \text{ mm}^3$ MgO substrates. The degree of grain coupling was tuned by controlling the O_2 pressure during deposition and quantified by the dc resistivity ρ_{dc} in the normal state at 5 K. Using a Mach-Zehnder interferometer we measured the complex transmission \hat{t} of radiation at frequencies 3–18 cm^{-1} transmitted through the bilayer system and through a bare reference substrate, in order to disentangle Al and MgO contributions. Optical ^4He cryostats allowed cooling the sample to $T \geq 1.65 \text{ K}$ [38]. At the same time we

measured the dc resistance $R_{dc}(T)$ and define T_c as temperature where R_{dc} becomes immeasurably small. We examined nine samples with different resistivity values covering both sides of the SC dome, see Fig. 1(a). We measured \hat{t} of all samples in the normal state well above T_c and in the SC state at $T_{\text{base}} = 1.65 \text{ K}$, as well as the temperature dependence of \hat{t} for representative HR and LR samples. The frequency-dependent dynamical conductivity $\hat{\sigma}(\nu) = \sigma_1(\nu) + i\sigma_2(\nu)$ is calculated from the optical data using the Fresnel functions [38,39].

THz spectroscopy allows us to extract the fundamental energy scales of interest, Δ and J , from the measured $\sigma_1(\nu)$ and $\sigma_2(\nu)$. While the pair-breaking energy scale Δ fixes the threshold for optical absorption in $\sigma_1(\nu)$ below T_c , the superfluid stiffness J is connected to $\sigma_2(\nu)$. In the present samples, $\sigma_1(\nu)$ and $\sigma_2(\nu)$ can be adequately described by means of the Mattis-Bardeen (MB) equations for dirty superconductors [47]. The accuracy of the MB fit of $\sigma_1(\nu)$ and $\sigma_2(\nu)$ is shown in Figs. 1(b)–1(d) for representative samples covering the low- (sample 1), high- (sample 3), and optimal-resistivity (sample 2) regimes of the phase diagram. Even though the fit captures well the increase of conductivity at $\nu > 2\Delta/(hc)$ (where h is the Planck constant and c is the speed of light), it underestimates $\sigma_1(\nu)$ at low frequencies. Such an excess conductivity resembles the one observed, e.g., in disordered NbN and InO films [40,41] and in cuprate films [42], and is attributed to SC collective modes [41–46], not included in the MB theory. In the case of granular Al, where the Josephson coupling between grains is expected to be spatially inhomogeneous, this excess conductivity may be attributed to SC phase fluctuations, made optically active by disorder [43–45]. A more quantitative study goes beyond the scope of this work. The gap value $\Delta(T)$ extracted from the fit of $\sigma_1(\nu)$ is extrapolated to $T = 0$ assuming the BCS temperature dependence for $\Delta(T)/\Delta(0)$, where the ratio $\Delta(0)/k_B T_c$ (with k_B the Boltzmann constant) is not constrained to the weak-coupling value.

The superfluid stiffness J is determined from $\sigma_2(\nu)$, which is proportional to n_s/m^* [15,47], where n_s and m^* are the superfluid density and effective charge carrier mass. More specifically, we define

$$J = \frac{\hbar^2 n_s a}{4m^*} = 0.62 \times \frac{a}{\lambda^2} [K]. \quad (1)$$

Here a is a transverse length scale, expressed in \AA , λ is the penetration depth in μm , and $n_s/m^* = 1/\lambda^2 \mu_0 e^2$. In an isotropic three-dimensional (3D) system, the length scale a in Eq. (1) is the SC coherence length ξ_0 , which is the natural cutoff for phase fluctuations, while it is the film thickness in the two-dimensional (2D) limit. Measurements of the upper critical field in similar samples [48,49] gave an estimate of $\xi_0 \simeq 10 \text{ nm}$, while the analysis [47,49] of the paraconductivity above T_c indicates a 2D character with an effective 2D thickness for SC fluctuations of the order of $\simeq 15 \text{ nm}$ throughout the phase diagram. We compare the evolution of superfluid stiffness (1) in our samples by choosing a constant value $a = 10 \text{ nm}$, for the sake of simplicity. Once $n_s(T)$ is determined, the zero-temperature extrapolation follows from the two-fluid formula [47].

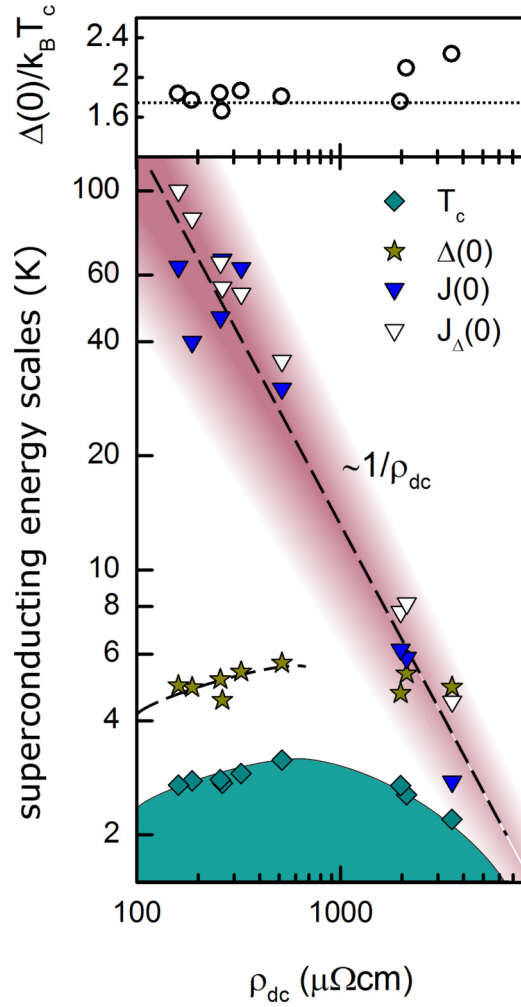


FIG. 2. Superconducting energy scales. T_c , $\Delta(0)$, $J(0)$, $J_{\Delta}(0)$ (expressed in units of temperature), and $\Delta(0)/k_B T_c$ as a function of normal-state resistivity (measured at 5 K) of granular Al films. T_c (green diamonds) encloses a superconducting dome with a maximum around $700 \mu\Omega \text{ cm}$ where T_c is enhanced by nearly a factor of 3 compared to the bulk value. $\Delta(0)$ (olive stars) follows the increase of T_c on the left side of the dome for LR samples while it saturates in the HR regime. This is reflected in the ratio $\Delta(0)/k_B T_c$ which increases from the weak-coupling value 1.78 (dotted line) to 2.25 when crossing from the left to the right side of the dome. The calculation of superfluid stiffness from $\sigma_2(\nu)$ and from $\Delta(0)$, i.e., $J(0)$ and $J_{\Delta}(0)$, is subject to an uncertainty reflected by the shaded area. $J(0)$ follows approximately a $1/\rho_{dc}$ behavior, as expected from Eq. (2) for a constant value of $\Delta(0)$, and becomes comparable to $\Delta(0)$ in the HR regime. Dashed lines are guides to the eye.

The above analysis was applied to all samples under study. Figure 2 comprises the results for the SC properties T_c , $\Delta(0)$, $J(0)$, and $\Delta(0)/k_B T_c$ and presents them as functions of the normal-state resistivity. With increasing resistivity, T_c is first elevated from 2.7 K to a maximum of 3.15 K before it is suppressed to 2.2 K. This SC dome with a maximum at about $700 \mu\Omega \text{ cm}$ is in agreement with previous works on granular Al composed of 2 nm grains [48,50,51]. The enhancement of T_c in the LR regime is accompanied by a concomitant increase of $\Delta(0)$, such that the ratio $\Delta(0)/k_B T_c$ remains around the weak-coupling value 1.78 for all LR samples. This behavior

is in contrast to the usual suppression of both T_c and $\Delta(0)$ for intermediate (but not too strong) disorder in homogeneously disordered films of conventional superconductors [25–30]. Thus, our measurements provide an experimental confirmation that in granular Al the T_c enhancement is due to an increase of the local pairing scale Δ in each grain by finite-size effects, as suggested by several theoretical works in the past [9–13,17]. However, as the dc resistance increases further, phase fluctuations become more prominent and the overall T_c of the array is suppressed, even though a large local pairing survives. This is demonstrated in the upper panel of Fig. 2, where $\Delta(0)/k_B T_c$ is shown to increase up to around 2.25 in the HR regime, i.e., T_c is reduced more strongly than the fairly constant $\Delta(0)$.

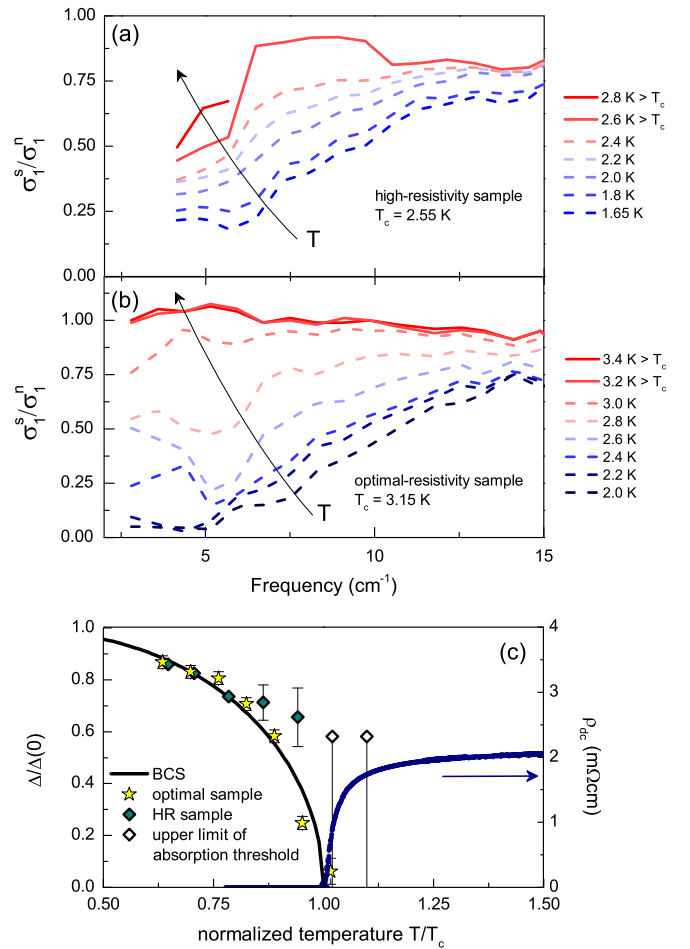


FIG. 3. Temperature evolution of spectral gap. (a) and (b) Temperature dependence of normalized $\sigma_1(\nu)$ of a granular Al sample in the high- and optimal-resistivity regimes [samples 2 and 3 in Fig. 1(d)]. In case of the HR sample, the suppression of $\sigma_1(\nu)$ below $T_c = 2.55 \text{ K}$ (dashed lines) persists up to $T = 2.8 \text{ K}$ (solid lines), whereas the spectral gap closes right at T_c in the LR regime. (c) Temperature dependence of the spectral gap for samples from the optimal (stars, sample 2) and high resistivity regimes (diamonds, sample 3). The blue data traces $\rho_{dc}(T)$ of the HR sample. For the HR sample, deviations from the BCS prediction for $\Delta(T)/\Delta(0)$ (black solid line) appear already at $T/T_c \lesssim 1$, where Δ is anomalously large. The persistence of a gap across T_c (empty diamonds) is in striking resemblance with strongly disordered or correlated superconductors.

The crossover to a SC transition driven by the loss of phase coherence in the HR samples is confirmed by the suppression of $J(0)$, shown in Fig. 2. The approximate scaling of $J(0)$ with ρ_{dc}^{-1} can be understood within the MB framework, where $J(0)$ is related to $\Delta(0)$ obtained from $\sigma_1(\nu)$ and the normal-state resistivity

$$J_{\Delta}(0) = \frac{R_c}{R_{sq}} \frac{\pi \Delta(0)}{4}, \quad (2)$$

where $R_c = \hbar/e^2$ and $R_{sq} = \rho_{dc}/a$ with same scale a as used in Eq. (1). Using $\Delta(0)$ extracted from σ_1 we calculate a stiffness $J_{\Delta}(0)$ that is similar to $J(0)$ extracted from $\sigma_2(\nu)$ following Eq. (1), see Fig. 2. The slightly different values of $J(0)$ and $J_{\Delta}(0)$ are reflected in the shaded area in Fig. 2. As the grains are progressively decoupled, the $1/\rho_{dc}$ prefactor in Eq. (2) varies strongly, dominating the overall scaling of $J(0)$. Even in the LR regime the absolute value of $J(0)$ is considerably lower than what is expected for ordinary superconductors, where $J(0)$ scales with E_F .

We find further evidence for an unconventional behavior of superconductivity from the dissipative conductivity. Figures 3(a) and 3(b) compare (normalized) $\sigma_1(\nu)$ spectra of high- and optimal-resistivity samples (samples 2 and 3 in Fig. 1) at various temperatures below (dashed lines) and above (solid lines) T_c . In the HR regime, MB theory agrees with the measured data at low temperatures [47], whereas by approaching T_c the data deviate significantly from the MB prediction, with a strong suppression of $\sigma_1(\nu)$ at low frequencies, see Fig. 3(a). This suppression in $\sigma_1(\nu)$ exists even at $T = 2.8$ K well above the SC transition, as evident from Fig. 3(c) where $\rho_{dc}(T)$ of the HR sample is shown for comparison. In contrast, for of the optimal-resistivity sample [Fig. 3(b)] both $\sigma_1(\nu)$ and \hat{t} spectra [47] contain no signs of a spectral gap above T_c , and $\Delta(T)$ follows closely the BCS temperature dependence, see Fig. 3(c). For the HR sample the quality of the MB fit degrades already at $T/T_c \simeq 0.8$, as signaled by the larger error bars in $\Delta(T)$ reported in Fig. 3(c), and $\Delta(T)$ evolves smoothly into a finite gap found

up to the highest measured temperature. The same anomalies are observed in the analysis of the paraconductivity that deviates [47] in the HR regime from the ordinary Aslamazov-Larkin type of Gaussian SC fluctuations, in agreement with previous observations based on magnetotransport and Nernst effect [48]. All these findings suggest that the anomalous T dependence of Δ and $\sigma_1(\nu)$ for HR samples near T_c can be attributed to a pseudogap above T_c , which can be viewed as a natural consequence of the phase-driven transition, even though a full theoretical understand of it is still lacking.

In conclusion, from our measurements of the dynamical conductivity of superconducting granular Al thin films at THz frequencies we determined the dependence of the energy scales T_c , $\Delta(0)$, and $J(0)$ on the decoupling of the Al grains. We show that decoupling promotes the individual nature of the grains and enhances the local pairing amplitude in each grain due to finite-size effects. The enhancement of both T_c and $\Delta(0)$ in the low-resistivity regime is eventually overcompensated in high-resistivity samples by enhanced phase fluctuations, which suppress T_c while the pairing amplitude remains large. The strong suppression of $J(0)$ and the persistence of a spectral gap above T_c in the high-resistivity regime indicate a crossover to a phase-driven transition. Our results show that granular Al is a perfect model system to elucidate the competition between pairing, superfluid coherence, and inhomogeneity that are common phenomena in the present field of superconductivity, and identify the general setup to achieve full control of the T_c enhancement via engineered nanoinhomogeneities.

We acknowledge discussions with Ya. Fominov, A. Frydman, and A. Garcia-Garcia. U.S.P. appreciates financial support from the Studienstiftung des deutschen Volkes. We acknowledge financial support from the German-Israeli Foundation for Scientific Research and Development (GIF Grant No. I-1250-303.10/2014). L.B. acknowledges financial support by Italian MIUR under projects FIRB-HybridNanoDev-RBFR1236VV, PRIN-RIDEIRON-2012X3YFZZ, and Premiali-2012 ABNAN-OTTECH. N.B. and U.S.P. contributed equally to this work.

-
- [1] D. M. Broun, *Nat. Phys.* **4**, 170 (2008).
 [2] N. D. Mathur, F. M. Frosche, S. R. Julian, I. R. Walker, D. M. Freye, R. K. W. Haselwimmer, and G. G. Lonzarich, *Nature (London)* **394**, 39 (1998).
 [3] A. D. Caviglia, S. Gariglio, N. Reyren, D. Jaccard, T. Schneider, M. Gabay, S. Thiel, G. Hammerl, J. Mannhart, and J. M. Triscone, *Nature (London)* **456**, 624 (2008).
 [4] D. C. Johnston, *Adv. Phys.* **59**, 803 (2010).
 [5] A. P. Drozdov, M. I. Erements, I. A. Troyan, V. Ksenofontov, and S. I. Shylin, *Nature (London)* **525**, 73 (2015).
 [6] B. Abeles, R. W. Cohen, and G. W. Cullen, *Phys. Rev. Lett.* **17**, 632 (1966).
 [7] R. W. Cohen and B. Abeles, *Phys. Rev.* **168**, 444 (1968).
 [8] G. Deutscher, M. Gershenson, E. Grunbaum, and Y. Imry, *J. Vac. Sci. Technol.* **10**, 697 (1973).
 [9] R. H. Parmenter, *Phys. Rev.* **166**, 392 (1968).
 [10] M. D. Croitoru, A. A. Shanenko, and F. M. Peeters, *Phys. Rev. B* **76**, 024511 (2007).
 [11] V. Z. Kresin and Y. N. Ovchinnikov, *Phys. Rev. B* **74**, 024514 (2006).
 [12] A. M. García-García, J. D. Urbina, K. Richter, E. A. Yuzbashyan, and B. L. Altshuler, *Phys. Rev. B* **83**, 014510 (2011).
 [13] Z. Lindemfeld, E. Eisenberg, and R. Lifshitz, *Phys. Rev. B* **84**, 064532 (2011).
 [14] A. M. García-García, J. D. Urbina, E. A. Yuzbashyan, K. Richter, and B. L. Altshuler, *Phys. Rev. Lett.* **100**, 187001 (2008).
 [15] V. J. Emery and S. A. Kivelson, *Nature (London)* **374**, 434 (1994).
 [16] S. Bose, A. M. Garcia-Garcia, M. M. Ugeda, J. D. Urbina, C. H. Michaelis, I. Brihuega, and K. Kern, *Nat. Mater.* **9**, 550 (2010).
 [17] J. Mayoh and A. M. García-García, *Phys. Rev. B* **90**, 134513 (2014).

- [18] V. F. Gantmakher and V. T. Dolgoplov, *Phys. Usp.* **53**, 1 (2010).
- [19] Y. H. Lin, J. Nelson, and A. M. Goldman, *Physica C* **514**, 130 (2015).
- [20] L. Merchant, J. Ostrick, R. P. Barber, and R. C. Dynes, *Phys. Rev. B* **63**, 134508 (2001).
- [21] M. D. Stewart, A. Yin, J. M. Xu, and J. M. Valles, *Science* **318**, 1273 (2007).
- [22] S. Eley, S. Gopalakrishnan, P. M. Goldbart, and N. Mason, *Nat. Phys.* **8**, 59 (2012).
- [23] Z. Han, A. Allain, H. Arjmandi-Tash, K. Tikhonov, M. Feigel'man, B. Sacépé, and V. Bouchiat, *Nat. Phys.* **10**, 380 (2014).
- [24] J. Biscara, N. Bergeal, S. Hurand, C. Feuillet-Palma, A. Rastogi, R. C. Budhani, M. Grilli, S. Caprara, and J. Lesueur, *Nat. Mater.* **12**, 542 (2013).
- [25] B. Sacépé, C. Chapelier, T. I. Baturina, V. M. Vinokur, M. R. Baklanov, and M. Sanquer, *Phys. Rev. Lett.* **101**, 157006 (2008).
- [26] M. Mondal, A. Kamlapure, M. Chand, G. Saraswat, S. Kumar, J. Jesudasan, L. Benfatto, V. Tripathi, and P. Raychaudhuri, *Phys. Rev. Lett.* **106**, 047001 (2011).
- [27] B. Sacépé, T. Dubouchet, C. Chapelier, M. M. Sanquer, M. Sanquer, D. Shahar, M. Feigel'man, and L. Ioffe, *Nat. Phys.* **7**, 239 (2011).
- [28] M. Chand, G. Saraswat, A. Kamlapure, M. Mondal, S. Kumar, J. Jesudasan, V. Bagwe, L. Benfatto, V. Tripathi, and P. Raychaudhuri, *Phys. Rev. B* **85**, 014508 (2012).
- [29] A. Kamlapure, T. Das, S. C. Ganguli, J. B. Parmar, B. S., and P. Raychaudhuri, *Sci. Rep.* **3**, 2979 (2013).
- [30] Y. Noat, V. Cherkez, C. Brun, T. Cren, C. Carbillat, F. Debontridder, K. Il'in, M. Siegel, A. Semenov, H.-W. Hübers, and D. Roditchev, *Phys. Rev. B* **88**, 014503 (2013).
- [31] D. Abraham, G. Deutscher, R. Rosenbaum, and S. Wolf, *J. Phys. Colloques* **39**, C6-586 (1978).
- [32] M. Gershenson and W. McLean, *Low Temp. Phys.* **47**, 123 (1982).
- [33] K. Steinberg, M. Scheffler, and M. Dressel, *Phys. Rev. B* **77**, 214517 (2008).
- [34] N. Bachar, U. Pracht, E. Farber, M. Dressel, G. Deutscher, and M. Scheffler, *J. Low Temp. Phys.* **179**, 83 (2014).
- [35] R. C. Dynes, J. P. Garno, G. B. Hertel, and T. P. Orlando, *Phys. Rev. Lett.* **53**, 2437 (1984).
- [36] C. T. Black, D. C. Ralph, and M. Tinkham, *Phys. Rev. Lett.* **76**, 688 (1996).
- [37] D. C. Ralph, C. T. Black, and M. Tinkham, *Phys. Rev. Lett.* **78**, 4087 (1997).
- [38] U. S. Pracht, E. Heintze, C. Clauss, D. Hafner, R. Bek, D. Werner, S. Gelhorn, M. Scheffler, M. Dressel, D. Sherman, B. Gorshunov, K. S. Il'in, D. Henrich, and M. Siegel, *IEEE Trans. Terahertz Sci. Technol.* **3**, 269 (2013).
- [39] M. Dressel and G. Grüner, *Electrodynamics of Solids—Optical Properties of Electrons in Matter* (Cambridge University Press, Cambridge, 2002).
- [40] R. W. Crane, N. P. Armitage, A. Johansson, G. Sambandamurthy, D. Shahar, and G. Grüner, *Phys. Rev. B* **75**, 094506 (2007).
- [41] D. Sherman, U. S. Pracht, B. Gorshunov, S. Poran, J. Jesudasan, M. Chand, P. Raychaudhuri, M. Swanson, N. Trivedi, A. Auerbach, M. Scheffler, and M. Dressel, *Nat. Phys.* **11**, 188 (2015).
- [42] J. Corson, J. Orenstein, S. Oh, J. O'Donnell, and J. N. Eckstein, *Phys. Rev. Lett.* **85**, 2569 (2000).
- [43] S. Barabash, D. Stroud, and I.-J. Hwang, *Phys. Rev. B* **61**, R14924 (2000).
- [44] T. Cea, D. Bucheli, G. Seibold, L. Benfatto, J. Lorenzana, and C. Castellani, *Phys. Rev. B* **89**, 174506 (2014).
- [45] M. Swanson, Y. L. Loh, M. Randeria, and N. Trivedi, *Phys. Rev. X* **4**, 021007 (2014).
- [46] T. Cea, C. Castellani, G. Seibold, and L. Benfatto, *Phys. Rev. Lett.* **115**, 157002 (2015).
- [47] See Supplemental Material at <http://link.aps.org/supplemental/10.1103/PhysRevB.93.100503> for more details.
- [48] S. Lerer, N. Bachar, G. Deutscher, and Y. Dagan, *Phys. Rev. B* **90**, 214521 (2014).
- [49] G. Deutscher and S. A. Dodds, *Phys. Rev. B* **16**, 3936 (1977).
- [50] N. Bachar, S. Lerer, A. Levy, S. Hacoheh-Gourgy, B. Almog, H. Saadaoui, Z. Salman, E. Morenzoni, and G. Deutscher, *Phys. Rev. B* **91**, 041123 (2015).
- [51] N. Bachar, S. Lerer, S. Hacoheh-Gourgy, B. Almog, and G. Deutscher, *Phys. Rev. B* **87**, 214512 (2013).